

## Antiferromagnetism in ZnSe/MnSe strained-layer superlattices

N. Samarth, P. Kłosowski,\* H. Luo, T. M. Giebułtowicz,\* and J. K. Furdyna  
*Department of Physics, University of Notre Dame, Notre Dame, Indiana 46556*

J. J. Rhyne

*University of Missouri Research Reactor, Columbia, Missouri 75211  
 and National Institute of Standards and Technology, Gaithersburg, Maryland 20899*

B. E. Larson

*Thinking Machines Corporation, Cambridge, Massachusetts 02215*

N. Otsuka

*School of Materials Engineering, Purdue University, West Lafayette, Indiana 47907  
 (Received 21 February 1991; revised manuscript received 22 May 1991)*

Neutron diffraction studies of ZnSe/MnSe strained-layer superlattices with individual MnSe layer thicknesses ranging from 3 to 15 monolayers show a second-order transition to type-III antiferromagnetic order. The magnetic reflections indicate a single orientation of the type-III domain, with the tetragonal axis perpendicular to the layer plane and the spins lying within the layer plane.

The fabrication by molecular-beam epitaxy (MBE) of low-dimensional structures containing layers of magnetic semiconductors (MS) has stimulated a variety of experimental studies on magnetic and magneto-optical phenomena in *diluted* magnetic semiconductor (DMS) systems such as ZnTe/Cd<sub>1-x</sub>Mn<sub>x</sub>Se.<sup>1</sup> Few studies have dealt with structures such as ZnSe/MnSe and CdTe/MnTe in which strained *zinc-blende* layers of an *undiluted* MS are stabilized by nonmagnetic layers.<sup>2,3</sup> From our detailed knowledge of zinc-blende DMS alloys and the only bulk-grown zinc-blende Mn chalcogenide  $\beta$ -MnS,<sup>4</sup> we expect these MS layers to be type-III Heisenberg antiferromagnets<sup>5-7</sup> governed by a dominant *short-ranged* antiferromagnetic superexchange<sup>8</sup> and a weaker Dzyaloshinskii-Moriya (DM) contribution.<sup>9</sup> MS superlattices hence offer an opportunity to systematically study the effects of strain and dimensional crossover in frustrated Heisenberg antiferromagnets. Further, superlattices containing isolated MS monolayers can provide physical realizations of frustrated two-dimensional (2D) XY antiferromagnets of current theoretical interest.<sup>10</sup> Finally, we note that the only other reported antiferromagnetic multilayer system with short-ranged interactions is FeF<sub>2</sub>/CoF<sub>2</sub>,<sup>11</sup> which involves Ising antiferromagnetism.

In this paper, we use neutron diffraction to obtain a detailed picture of antiferromagnetism in a prototypical MS superlattice (ZnSe/MnSe). While early magneto-optical and magnetization studies of ZnSe/MnSe superlattices *suggested* antiferromagnetic behavior in MnSe layers for thicknesses > 3 monolayers,<sup>2,12</sup> detailed information about the antiferromagnetic phase of MS superlattices (e.g., the Néel temperature and the magnetic structure) has never been reported. Our neutron-diffraction measurements *directly* show type-III antiferromagnetic order in MnSe layers down to thicknesses of 3 monolayers. As shown in Fig. 1, only *one* orientation of the tetragonal type-III domain is found with the tetragonal axis *parallel*

to the growth direction, and with the spins lying in the layer plane. In contrast, polycrystalline samples of  $\beta$ -MnS and isotropic single crystals of DMS alloys show three equivalent domain orientations. Further, we believe that the strained MnSe layers show a *second-order* phase transition, in contrast to the only other undiluted, zinc-blende type-III antiferromagnet studied so far ( $\beta$ -MnS) which shows a *first-order* transition.<sup>5</sup>

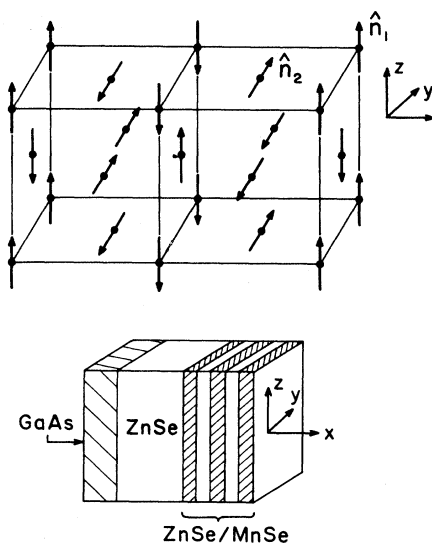


FIG. 1. Type-III magnetic unit cell in ZnSe/MnSe superlattices deduced from diffraction studies, showing the unique orientation of the tetragonal magnetic unit cell relative to the sample geometry. The spin axis lies in the  $y$ - $z$  plane as shown, but the spins at  $x=0, \frac{1}{2}$  (characterized by  $\hat{n}_1$ ) can be rotated an arbitrary but equal amount with respect to those at  $x=\frac{1}{4}, \frac{3}{4}$  (characterized by  $\hat{n}_2$ ). Anisotropic DM exchange favors the noncollinear spin arrangement shown (Ref. 6).

The samples used in this study were fabricated by MBE. The ZnSe/MnSe superlattices were grown on (100) GaAs wafers (typically, 2–3 cm<sup>2</sup> in area) at a substrate temperature of 320 °C, after first depositing a 5000 Å buffer layer of ZnSe. The sample surface was monitored by *in situ* reflection high-energy electron diffraction (RHEED) at 10 keV. By monitoring oscillations in the intensity of the specular spot in the RHEED pattern along the [011] azimuth, superlattice periods can be precisely timed in integral numbers of monolayers. The structure of the five samples studied is described by the specific parameters listed in Table I, and exemplified in Fig. 1. Transmission electron microscopy (TEM) clearly shows the formation of uniform superlattice structures with well-defined interfaces.

Neutron-diffraction measurements were carried out at the 20-MW research reactor of the National Institute of Standards and Technology using a triple axis spectrometer with a (002) pyrolytic graphite (PG) monochromator and analyzer, and a PG filter in the incident beam. An analyzer fixed for elastic scattering was used to reduce the large inelastic incoherent background from the GaAs substrate. The energy used was 13.7 and 14.8 meV with 40' collimation throughout the spectrometer for most of the data. The growth direction is taken to be [100] and the epilayer plane to be (100). The samples were placed in a variable-temperature cryostat, and were oriented with the scattering plane coincident with the (001) crystal plane, hence allowing the observation of the (*hk*0) reflections.

Scans through the (200) nuclear reflection along the [100] direction revealed several well-resolved satellite peaks characteristic of the superlattice periodicity, with Bragg peaks occurring at regular intervals  $2\pi/D$  in *Q* space (where *D* is the superlattice period). The period inferred from the satellite peaks is in good agreement with that expected from the RHEED oscillations and is also confirmed by TEM studies. A detailed analysis of the nuclear scans is given elsewhere.<sup>13</sup>

In all our samples, below a critical temperature  $T_N$  additional diffraction maxima are observed corresponding to type-III antiferromagnetic superstructure points. Of all the possible type-III reflections,<sup>7</sup> we observe only those corresponding to the domain with the tetragonal axis along [100]. Representative data for three different samples are shown in Fig. 2, where the scans for the ( $\frac{1}{2}$ , 1, 0) reflection along the *x* and *y* direction are shown as a function of the *Q* vector. The scans along [010] show long-range order in the plane of the layers with a range > 500 Å, while the scans along [100] show that—as might be expected—the correlation range along the growth direc-

TABLE I. Summary of samples used in the experiments.

Sample	ZnSe thickness (monolayers)	MnSe thickness (monolayers)	Periods
SL-20	20	15	100
SL-17	20	10	100
SL-22	12	7	200
SL-40	10	5	200
SL-42	6	3	500

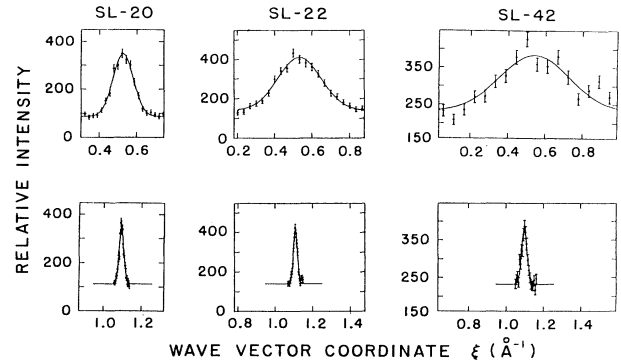


FIG. 2. In the upper and lower panels, we show scans along the [100] and [010] directions, respectively, of the ( $\frac{1}{2}$ , 1, 0) magnetic peak in three of the samples. The peak widths are inversely related to the order range in their respective crystallographic directions. The [010] scan gives a correlation length of at least 500 Å within the *y-z* plane. The [100] scan shows the extent of AFM-III in the *x* direction to be equal to the MnSe layer thickness.

tion simply corresponds to the MnSe layer thickness. Remarkably, long-range order within the plane is found even in the sample with 3 monolayers of MnSe. Further, following standard analysis,<sup>5</sup> the relative intensities of different type-III reflections clearly indicate that the spins are confined to the *y-z* plane (Table II). We cannot directly distinguish between a collinear arrangement of spins and the noncollinear arrangement shown in Fig. 1. However, the presence of a single domain orientation provides a favorable situation<sup>5</sup> for future experiments addressing this issue.

The stabilization of a unique domain orientation is a direct consequence of strain. There is a 4% lattice mismatch between ZnSe ( $a=5.667$  Å) and MnSe ( $a=5.91$  Å), with the strain being accommodated by elastic deformation. Neutron-diffraction measurements of the in-plane and perpendicular lattice parameters (*a* and *c*, respectively) of the MnSe layers show a compression of the former and an expansion of the latter, with a resulting tetragonal distortion of the MnSe layers of around  $(a-c)/a=6\%$ .<sup>13</sup> This tetragonal distortion results in different exchange interactions for directions parallel and

TABLE II. Integrated intensities of (*hk*0) magnetic reflections from SL-22 compared with calculated intensities for two different models.

Reflection indices ( <i>hkl</i> )	Intensity <sup>a</sup>	Intensity <sup>b</sup>	Intensity <sup>c</sup>
$\frac{1}{2}$ , 1, 0	6.9 ± 0.5	5.7	9.0
$\frac{3}{2}$ , 1, 0	5.9 ± 0.5	5.9	2.5
$\frac{5}{2}$ , 1, 0	4.2 ± 0.4	3.6	0.7
$\frac{1}{2}$ , 3, 0	0.9 ± 0.3	1.6	3.7
$\frac{3}{2}$ , 3, 0	1.1 ± 0.2	1.5	2.3

<sup>a</sup>Experiment.

<sup>b</sup>Spins in *y-z* plane.

<sup>c</sup>Spins along *x*.

perpendicular to the epilayer plane ( $J_{\parallel}$  and  $J_{\perp}$ , respectively). The interaction energy per spin for the domain with the tetragonal axis along [100] is then  $-8J_{\parallel}$ , while that for the two domains with the tetragonal axis in the (100) plane is  $-8J_{\perp}$ . Hence, the single domain orientation is consistent with  $J_{\parallel}$  being larger than  $J_{\perp}$ .

The temperature dependence of the intensity of magnetic reflections is shown in Fig. 3. For samples with MnSe layer thickness  $\geq 5$  monolayers, the data can be fitted reasonably well by a squared Brillouin function, consistent with a second-order phase transition in the mean-field approximation. At this stage, more detailed analysis of critical behavior is not possible because of insufficient scattered intensity in the critical region due to the small volume of magnetic material.

The Néel temperature for the 5–20 monolayer samples decreases slightly but noticeably (from 115 to 95 K) with decreasing layer thickness, suggesting a dimensional crossover regime from  $d=3$  to  $d=2$ . The Brillouin fit for the 3 monolayer sample is also shown for completeness. While the data is of poorer statistical quality, this sample clearly shows a drastic lowering of the Néel temperature to about 75 K. Here, however, it is difficult to disentangle intrinsic dimensional effects from extrinsic factors such as interfacial disorder due to interdiffusion and fractional coverage steps.

Since the phase transition in our system is not completely characterized, we refrain from a detailed theoretical analysis of the above observations. However, our

knowledge of the magnetic interactions in MS is complete enough<sup>8,9</sup> to propose a *plausible* model that is *consistent* with the experimental data. Consider a single isolated magnetic period of the strained superlattice. The strained type-III ground states may be completely specified by the unit vectors  $\mathbf{n}_1$  and  $\mathbf{n}_2$  characterizing the staggered magnetizations on two *independent* sets of planes as shown in Fig. 1. The long-wavelength exchange energy (per spin) may be written

$$\mathcal{H}_{\text{ex}} = \rho \int d^d x \{ (\nabla \mathbf{n}_1)^2 + (\nabla \mathbf{n}_2)^2 + A [ (\partial_x \mathbf{n}_1)^2 + (\partial_x \mathbf{n}_2)^2 ] \},$$

where  $\rho$  represents spin stiffness and  $A$  characterizes its lattice anisotropy. The exchange energy is purely isotropic in spin space, so  $\mathcal{H}_{\text{ex}}$  must be rotationally invariant. In the absence of anisotropic interactions, the ground state has a continuous degeneracy because the exchange energy does not depend on terms such as  $(\mathbf{n}_1 \cdot \mathbf{n}_2)^2$  which couple the two sets of planes.

In addition, the strain induces a single-ion anisotropy term,<sup>14</sup>

$$\mathcal{H}_{XY} = D \int d^d x (n_{1x}^2 + n_{2x}^2).$$

Our calculation yields an easy *plane* anisotropy, in contrast to the easy *axis* anisotropy predicted by Jackson in DMS superlattices.<sup>15</sup> We also need to add the DM anisotropic exchange,<sup>6,9</sup>

$$\mathcal{H}_{\text{DM}} = -\Delta_{\text{DM}} \int d^d x \hat{\mathbf{x}} \cdot (\mathbf{n}_1 \times \mathbf{n}_2).$$

Both the single-ion and DM anisotropies confine the staggered magnetizations to the  $y$ - $z$  plane, in agreement with our experimental findings. Further, the DM anisotropy partially lifts the type-III degeneracy by selecting a value for  $\mathbf{n}_1 \times \mathbf{n}_2$  (e.g., along  $\hat{\mathbf{x}}$ ).<sup>6</sup> Both the single-ion and DM terms are invariant under rotations of  $\mathbf{n}_1$  and  $\mathbf{n}_2$  *together* in the  $y$ - $z$  plane, leaving a single degree of freedom in the plane,  $\mathbf{N} \equiv \mathbf{n}_1$  (or equivalently  $\mathbf{n}_2$ ). The system hence has an  $XY$  order parameter, and should exhibit a continuous transition in  $d=3$ . (We recall that cubic  $\beta$ -MnS shows a *first-order* transition, consistent with renormalization-group calculations for an  $n=6$  order parameter.) As layer thickness is decreased towards  $d=2$ , our systems should exhibit a continuous Kosterlitz-Thouless-like transition.<sup>16</sup> While the details of such a crossover regime can be complicated by the presence of small interlayer couplings, fourfold in-plane anisotropies and nonuniform strain distributions, one might expect such a system to show a Néel temperature proportional to layer thickness, as is observed in liquid-He films.<sup>16</sup> It is premature to speculate more until further experimental information is obtained about the critical behavior (i.e., critical exponents). It is important to point out, however, that it is unlikely that the observed transition arises simply from the smearing of a first-order transition by a nonuniform strain distribution. The variation in lattice parameter from inhomogeneous strain is easily estimated from the deconvoluted width of nuclear peaks observed in longitudinal scans; we find that the spread in the lattice param-

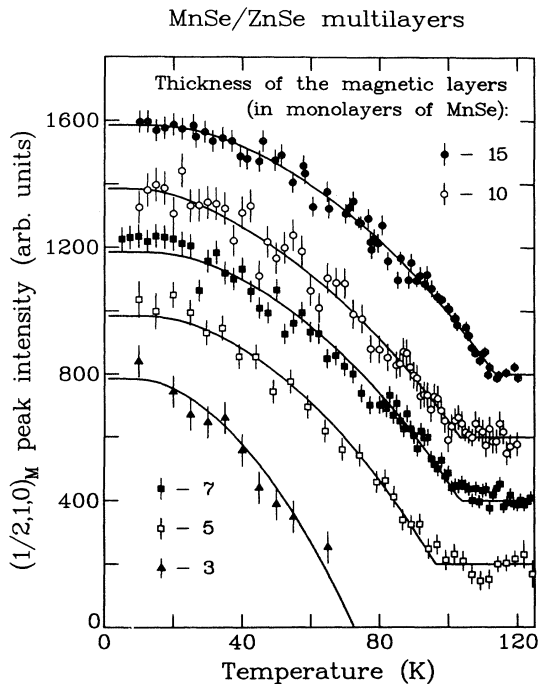


FIG. 3. Temperature dependence of the intensity of the  $(\frac{1}{2}, 1, 0)$  magnetic reflection for all the samples studied. The intensity is proportional to the square of the staggered magnetization, and the data are fitted to the square of a Brillouin function in the mean-field approximation.

eter is 0.02–0.025 Å, which is much smaller than the lattice distortion itself (typically, 0.15–0.20 Å). We hence conclude that the lowering of symmetry affects the phase transition far more significantly than inhomogeneous strain.

In conclusion, neutron-diffraction measurements have provided a picture of the antiferromagnetic ordering in an MS superlattice. These are detailed magnetic studies of a different class of strained, multilayer Heisenberg antiferromagnets. Studies are already underway on several other MS superlattices (ZnTe/MnTe, ZnTe/MnSe, and

CdTe/MnTe) which offer a rich variety of strain configurations in which to systematically study magnetic ordering and phase transitions as a function of the strain field.

We thank U. Debska for the purification of the source materials and are grateful to R. L. Gunshor for advice about the growth of ZnSe/MnSe. This work was supported by National Science Foundation Grant No. DMR-8821635 and by ONR Grant No. N-00014-90-5-1782.

\*Currently at National Institute of Standards and Technology, Gaithersburg, MD 20899.

<sup>1</sup>D. D. Awschalom, M. R. Freeman, N. Samarth, H. Luo, and J. K. Furdyna, *Phys. Rev. Lett.* **66**, 1212 (1991), and references therein.

<sup>2</sup>L. A. Kolodziejski *et al.*, *Appl. Phys. Lett.* **48**, 1482 (1986).

<sup>3</sup>S. M. Durbin *et al.*, *Appl. Phys. Lett.* **55**, 2087 (1989).

<sup>4</sup>Bulk-grown MnSe and MnTe crystallize in the rocksalt and NiAs phases, respectively.

<sup>5</sup>J. Hastings, L. M. Corliss, W. Kunmann, and D. Mukamel, *Phys. Rev. B* **24**, 1388 (1981), and references therein.

<sup>6</sup>F. Keffer, *Phys. Rev.* **126**, 896 (1962).

<sup>7</sup>T. Giebultowicz *et al.*, *Phys. Rev. B* **42**, 2582 (1990), and references therein.

<sup>8</sup>B. E. Larson *et al.*, *Phys. Rev. B* **37**, 4137 (1988).

<sup>9</sup>B. E. Larson and H. Ehrenreich, *Phys. Rev. B* **39**, 1747 (1989).

<sup>10</sup>C. L. Henley, *Phys. Rev. Lett.* **62**, 2056 (1989).

<sup>11</sup>C. A. Ramos, D. Lederman, A. R. King, and V. Jaccarino, *Phys. Rev. Lett.* **65**, 2913 (1990).

<sup>12</sup>S. K. Chang *et al.*, *J. Appl. Phys.* **62**, 4835 (1987).

<sup>13</sup>P. Klosowski *et al.*, *J. Appl. Phys.* **69**, 6109 (1991).

<sup>14</sup>Tight-binding calculations for a 5-site Mn-centered cluster predict that the anisotropy constant  $D$  depends on the anion spin-orbit strength  $\lambda$  and the strain-induced  $c/a$  ratio as  $D \sim \lambda^2[(c/a)^2 - 1]$ . The cubic (fourfold) anisotropy within the  $y$ - $z$  plane should be negligible, at least away from an interfacial layer.

<sup>15</sup>S. A. Jackson, *Surf. Sci.* **228**, 230 (1990).

<sup>16</sup>J. M. Kosterlitz and D. J. Thouless, in *Progress in Low Temperature Physics*, edited by D. F. Brewer (North-Holland, Amsterdam, 1978), Vol. VII B, p. 373.